Technical University of Denmark

DTU

Empiric analysis of zero voltage switching in piezoelectric transformer based resonant converters

Rødgaard, Martin Schøler; Andersen, Thomas; Andersen, Michael A. E.

DTU Library
Technical Information Center of Denmark

EMPIRIC ANALYSIS OF ZERO VOLTAGE SWITCHING IN PIEZOELECTRIC TRANSFORMER BASED RESONANT CONVERTERS

M. S. Rødgaard *, T. Andersen*, M. A. E. Andersen*

*Technical University of Denmark, DTU Elektro, Ørsteds Plads, building 349, DK-2800 Kgs. Lyngby, Denmark,
msr@elektro.dtu.dk*

Keywords: Piezoelectric Transformer, inductor-less, converter, soft switching, ZVS factor

Abstract

Research and development within piezoelectric transformer (PT) based converters are rapidly increasing, as the technology is maturing and starts to prove its capabilities. High power density and high efficiencies are reported and recently several inductor-less converters have emerged [1][2][7][10][13], which demonstrates soft switching capabilities. The elimination of a bulky inductor, reduces size and price of the converter, but demands a soft switching optimised PT. Several attempts of expressing the soft switching capability have been made [5][12], with some shortcomings. The goal of this paper is to derive a simple expression of the maximal obtainable soft switching capability (ZVS factor), for a specific PT design, assuming a matched load. The expression has been derived through series of parametric sweep simulations of the inductor-less half-bridge topology, which revealed that a linearization of the maximal soft switching capability can be performed, in the area of interest. This expression is intended to form a basic tool for development of soft switching optimised PT's, which enables the utilisation of inductor-less topologies.

1 Introduction

Piezoelectric transformer (PT) based converters have been around for some time now, but within resent years PT based converters have emerged, that exploit an inductor-less topology [1][2][7][10][13]. The elimination of the bulky inductor reduces size and price of the converter. But the parasitic input capacitance of the PT usually prevents the utilisation of an inductor-less power stage and an external series inductance is typically inserted in order to achieve soft switching capabilities. In a simple half-bridge power stage the input capacitance can lead to hard switching losses in the same range as the output power, resulting in a very poor efficiency. This calls for other means in order to avoid large hard switching losses, obtain soft switching capabilities and efficient operation. This can be achieved by utilising an advantageous PT structure and optimised design. But in order to evaluate the properties of the PT, a better understanding of the PT and what factors influences the soft switching

capability is required. Several attempts of deriving a mathematical expression of the soft switching capability, directly from the lumped parameter model Figure 1 [11], have been made [3][5][10][12]. Great progress has been achieved, but they still have some shortcomings.
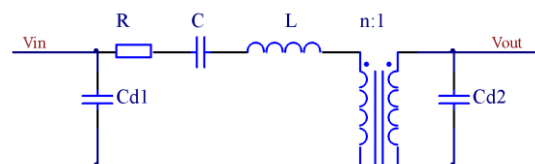

Figure 1: Lumped parameter model, which describes the behaviour of the PT in a narrow band around the operating resonance mode.

The approach in [5] has been to derive the full mathematical problem of the lumped parameter model, with respect to the input voltage, which should reach at least the half-bridge rail voltages, in order to soft switch. The result is a very precise expression of the soft switching capability. Its advantages are that it takes all the lumped parameters and the load resistance in to account, meaning that the soft switching capability can be calculated for any given PT and load, as well as the result is very accurate. The drawback of taking all the parameters and the load resistance in to account are a very complex expressing, making it quit computational heavy, as well as the expression still is a function of dead time and frequency. Furthermore there are no transparent relation between the parameters and the soft switching capability.

The approach in [12] has been to derive the expression in the frequency domain, as the lumped parameter model is of frequency domain nature. The derivation assuming matched load and has been accomplished by making a couple of assumptions. Equation 1 expresses the derived ZVS (zero voltage switching) factor, which is the maximal obtainable soft switching capability.

$$V_P^{'} = \frac{1}{n^2} \frac{C_{d2}}{C_{d1}} \frac{32\sqrt{6}}{9\pi^2} \eta \qquad (1)$$

It has the advantages of being very short and handy, as well as being transparent, providing a very good relation between the parameters and the ZVS factor. And as it can be seen, it is only a few parameter of the model that affects the ZVS factor.

The drawback is that it is too optimistic. Through employment of the expression, within PT development and experimental work, it is found that a ZVS factor of at least 1.4 is needed in order to achieve soft switching.

The approach of this paper has been to perform a series of parametric sweep simulations of the lumped parameter model, searching for linearization opportunities in respect to the soft switching capability. The ZVS factor Equation (1) has been the starting point for the simulations and search, as it has demonstrated to relate to the soft switching capability, although it is optimistic. And as this paper will demonstrate, linearization opportunities were found in the area of interest. As a result a simple expression of the ZVS factor is derived, which demonstrates good accuracy and is only a function of the input and output capacitor ratio and the efficiency, just as Equation (1).

1.1 Piezoelectric transformer

PT's are based on piezoelectric materials, which usually is a ceramic material. This material has an electromechanical coupling and through this coupling a charge displacement is generated, that is proportional to the deformation of the material. A PT is basically two piezoelectric elements joined together to form a transformer. The primary side element is then exited by an electrical AC voltage, which induces a deformation of the two joined elements. This deformation generates an output voltage on the secondary side element and through a proper design of the PT, a desired voltage conversion can be achieved from the primary to the secondary side.

The PT is operated in one of its resonance modes, in order to convert energy at a high efficiency [6][8][9][10]. The PT resonates each time it is possible to generate a standing wave in the element, but the design is usually optimised for one specific resonance mode, in order to achieve the highest efficiency [8][10].

The PT resembles a distributed network, but for simplicity and mathematical representation, only the resonance mode of interest is modelled [8][9][10]. The lumped parameter model is one of the most frequently used PT models and was derived by Mason in 1942 [11]. The model is illustrated in Figure 1 and is basically a LCC resonance tank, as well as the behaviour of a PT based converter is quite similar to a traditional resonance converter [4].

2 Inductor-less half-bridge

Figure 2 illustrates the inductor-less half-bridge topology, where the absence of a series inductance and the parasitic input capacitor C_{d1}, calls for a soft switching optimised PT. The topology is quite simple, making it easy to understand the subject of soft switching. But the soft switching requirements of the PT for a bit more advance topologies, like the full-bridge, are the same. However for the more advanced topologies, like the PFC charge pump topologies [7], the requirements to the soft switching capability of the PT are higher, as the apparent parasitic input capacitance is increased.

The PT is loaded with a matched load as this maximises the power transfer of the resonance network, as well as this is the worst case condition for the soft switching capability [12].
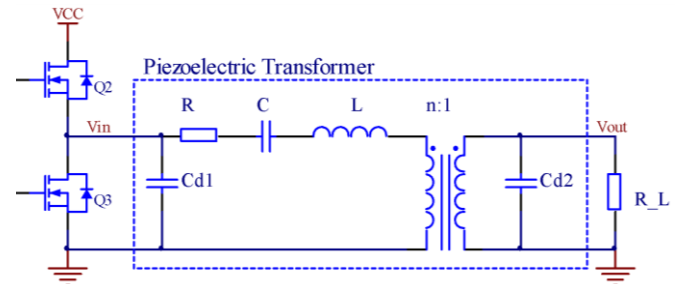
Figure 2: Schematical diagram of the inductor-less half-bridge topology and the PT equivalent lumped parameter model.

The target of soft switching is to achieve ZVS of the switches in the half-bridge. This can be achieved by operating the PT slightly above its resonance frequency, where the series resonance network becomes inductive and contains enough resonating energy to charge and discharge C_{d1}. And as it will be shown in the following section, there is an optimum where the resonance networks inductivity and energy is maximised, to make the largest energy transfer to C_{d1}. Furthermore there should be a certain dead time in between the two switches, in order to let the charge and discharge occur.
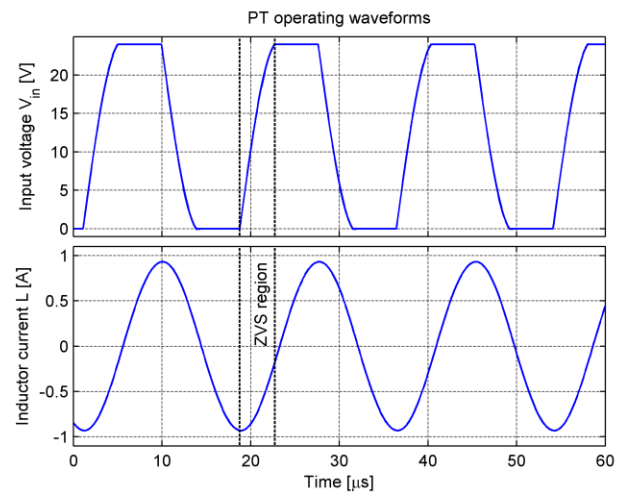
Figure 3: Input voltage and resonance current waveforms of the inductor-less half-bridge topology. From the input voltage it can clearly be seen that the half-bridge is operating under ZVS.

Figure 3 illustrates the operation of the inductor-less half-bride and as it can be seen the resonance current possesses sufficient phase shift and magnitude, to achieve ZVS. There is also sufficient dead time (ZVS region) in between the switches and it can clearly be seen that C_{d1} is charged and discharged, obtaining ZVS.

3 Soft switching factor

In the following section an expression of the maximal obtainable soft switching capability, also referred to as the soft switching factor or ZVS factor, is derived. The derivation is based on a series of parametric sweep time domain PSpice simulations of the inductor-less half-bridge, where the figures of Table 1 are the used lumped parameters. The figures origins from the interleaved multi layer Rosen-type PT design presented in [14], but as the lumped parameter mode is independent of PT design, the results should be general. The simulations have been preformed with at least 100 cycles before any measurements were made, in order to insure steady-state operation. Furthermore the simulated circuit utilises idealised switches and body diodes.

R	C	L	C_{d1}	C_{d2}	1/n
98mΩ	11.7nF	733µH	112nF	14.6pF	112

Table 1: FEM simulated PT equivalent lumped parameters obtained through impedance measurements.

From Equation (1) the ZVS factor of [12] can be calculated, as well as the match load and efficiency [12][14], as well as the resonance frequency. And as it can be seen from Table 2, the design possesses a ZVS factor which is sufficient to achieve soft switching.

$V'_{P\text{-Old}}$	R_{match}	η	f_R
1.43	198kΩ	0.987	55.2kHz

Table 2: FEM simulated PT equivalent lumped parameter model performance properties.

Equation (1) revealed that the soft switching capability is strongly dependent of the input and output capacitance. Figure 4 illustrates a frequency swept series of simulations, with the parameter of the input capacitance C_{d1} being swept as well.
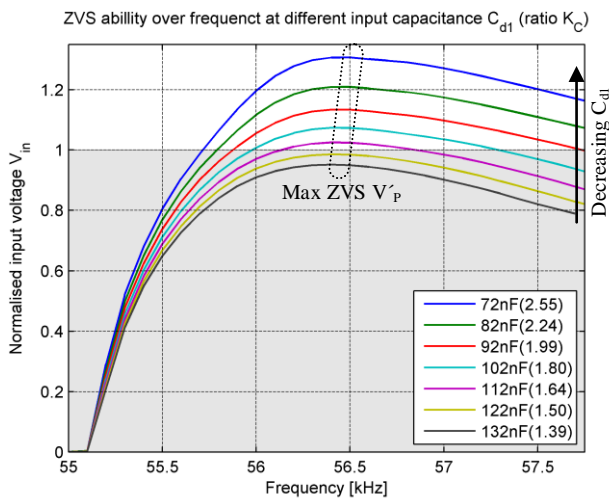

Figure 4: Simulated PT soft switching capability over frequency, with different input capacities Cd1 (capacitor ratio K_C).

As it can be seen the soft switching capability is strongly dependent of the input capacitance C_{d1} and the frequency. As for the shape of the curves there are a very good correlation to what were discovered in [5][12]. From the curves the maximal obtainable soft switching capability can be extracted, which is the parameter of interest. This ZVS factor can then be plotted in relation to the input capacitance C_{d1} or more interesting, in relations to the input and output capacitor ratio K_C Equation (2), which is illustrated in Figure 5.

$$K_C = \frac{1}{n^2}\frac{C_{d2}}{C_{d1}} \qquad (2)$$

The ZVS factors extracted from Figure 4 resemble the second topmost line in Figure 5. Moreover the series resistance R has been swept, creating several curves relating the ZVS factor to the PT efficiency.
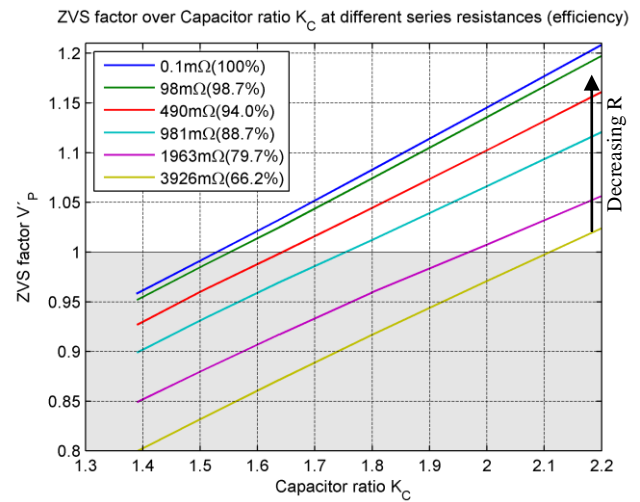

Figure 5: Simulated PT maximal soft switching capability (ZVS factor) in relation to the capacitor ratio K_C, at different efficiencies.

As Figure 5 reveals, there is a fine linear relation between the capacitor ratio K_C and the ZVS factor. By making a linear regression of the topmost line (η ≈ 100%), the most simplified expression of the ZVS factor is found Equation (3).

$$V'_{P\_100\%} = \left(0.304\frac{1}{n^2}\frac{C_{d2}}{C_{d1}} + 0.538\right) \qquad (3)$$

This expression is as simple as it gets, it is very handy and holds for high efficient PT's, which in the end is the ultimate goal of PT development.

But when working with less efficient PT's (< 97%), the efficiency should be taken in to account as well, in order to get a reliable result. Taking a look at Figure 5 it can be seen that the curves, which are lines of different efficiency, are nearly parallel. By taking a closer look at the curves it is found that they intersect the x-axis in roughly the same point, which indicates that the ZVS factor Equation (3) can be adjusted with an efficiency dependent factor.

Figure 6 illustrates how the ZVS factor is dependent on the efficiency at different capacitor ratios K_C and here as well the figure reveals a clear dependency of the efficiency. Although the dependency is not perfectly linear and differentiates a bit over the capacitor ratio K_C, a linear regression is made.
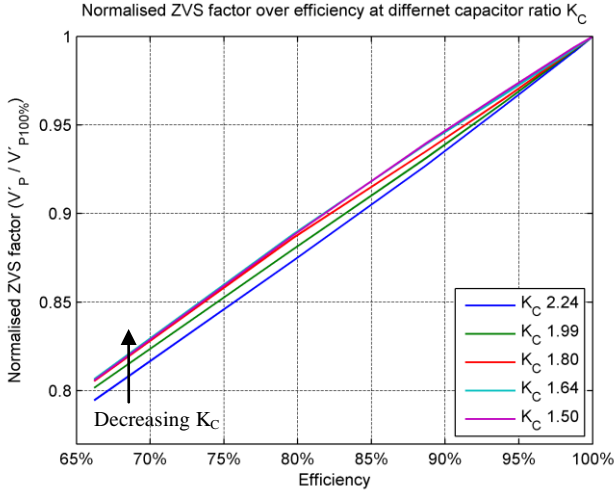

Figure 6: Simulated PT normalised maximal soft switching capability in relation to the efficiency.

The result is the correction factor Equation (4), which joined together with Equation (3) forms the final ZVS factor Equation (5).

$$K_\eta = (0.585\eta + 0.414) \qquad (4)$$

$$V'_P = \left(0.304\frac{1}{n^2}\frac{C_{d2}}{C_{d1}} + 0.538\right)(0.585\eta + 0.414) \quad (5)$$

The expression is verified through comparison with the already simulated data of Figure 5 and as can be seen in Table 3 there are a very good correlation.

4 Experimental results

In order to fully validate the developed ZVS factor, the ZVS factor of a prototype PT has been measured.
The prototype PT is of the same design as the one simulated [14], with the exception of a bit different polarisation, which divides the turn's ratio (n) by two. Its properties are listed in Table 4 and Table 5, and as it can be seen it possesses a quit high ZVS factor.

η = 100%			η = 94%			η = 80%		
Sim	V'$_P$	Δ	Sim	V'$_P$	Δ	Sim	V'$_P$	Δ
0,96	0,96	**0,1%**	0,93	0,93	**-0,1%**	0,85	0,85	**-0,5%**
0,99	0,99	**0,2%**	0,96	0,96	**-0,2%**	0,88	0,88	**-0,6%**
1,03	1,03	**0,2%**	1,00	1,00	**0,0%**	0,92	0,91	**-0,6%**
1,08	1,08	**0,1%**	1,04	1,05	**0,1%**	0,96	0,95	**-0,5%**
1,14	1,14	**0,0%**	1,10	1,10	**0,2%**	1,01	1,01	**0,1%**
1,22	1,22	**-0,3%**	1,17	1,17	**0,1%**	1,07	1,07	**0,6%**

Table 3: Comparison between some of the simulated and calculated ZVS factors.

R	C	L	C_{d1}	C_{d2}	1/n
361mΩ	8.33nF	1052µH	129nF	93.2pF	55

Table 4: Prototype PT equivalent lumped parameters obtained through impedance measurements. The measurements have been performed with the PT mounted in the test circuit, including the additional parasitic.

V'$_{P-Old}$	V'$_P$	R$_{match}$	η	f$_R$
1.67	1.15	33.7kΩ	0.936	54.2kHz

Table 5: Prototype PT equivalent lumped parameter model performance properties.

By employing the inductor-less half-bridge, it is not directly possible to measure ZVS factors above 1, because of the clamping body diodes in the MOSFET's. Only ZVS factor below 1 is measurable, as the measurement shown in Figure 8.
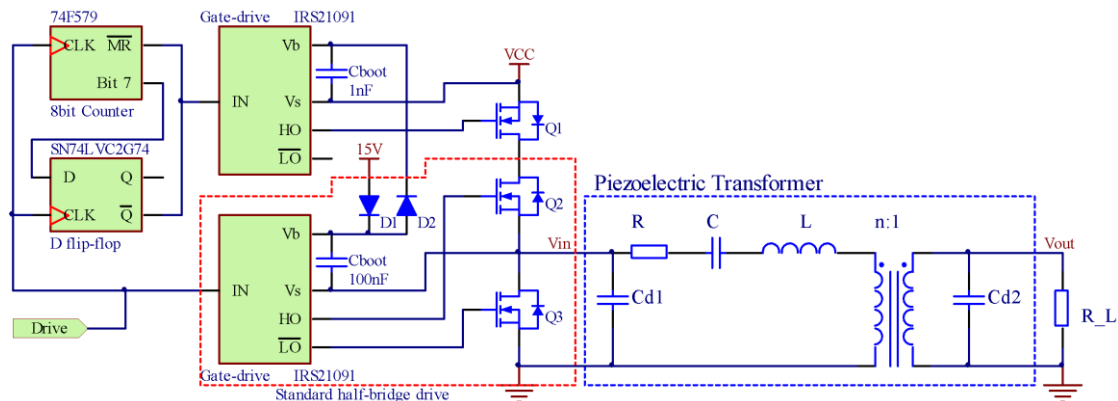

Figure 7: Schematical diagram of the inductor-less half-bridge, half-bridge driving circuit and the implemtatin of the soft switching capabability measurement circuit.

A diode could be placed in series with the top MOSFET and the input voltage (V_{in}) is thereby allowed to rise above supply voltage. This will enable a ZVS factor measurement, but it will also change the shape of the input voltage somewhat, changing the operation point. However by utilising a MOSFET instead of a diode, as in Figure 7 Q1, the input voltage is only allowed to rise above supply voltage once in a while. This is implemented as shown in Figure 7, with an N-channel MOSFET, a D flip-flop and a 8bit counter. The idea is to turn on Q1 and as Q2 and Q3 operates normally as a half-bridge, the counter counts the driving signal cycles. And when the counter reaches 256 cycles, the D flip-flop turns off Q1 for one cycle and resets the counter. In this manner the input voltage (V_{in}) is "released" and a ZVS factor higher than 1 can be measured, just as shown in Figure 9.
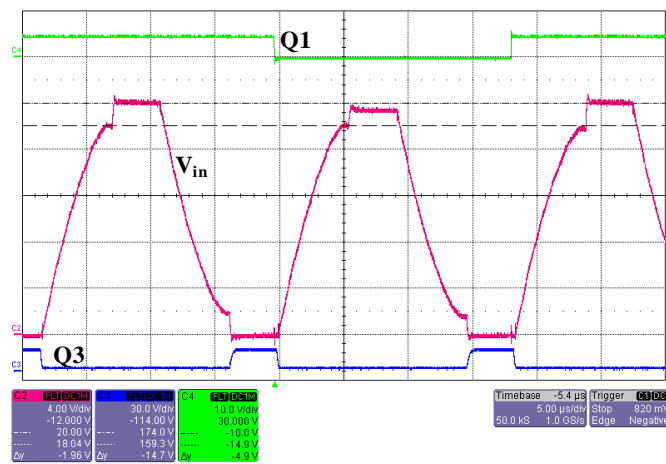

Figure 8: ZVS factor measurement of the prototype PT, with at capacitor ratio K_C of 1.38 (C_{d1} = 189nF). C3 and C4 shows gate signals, and C2 is the input voltage [4V/div].
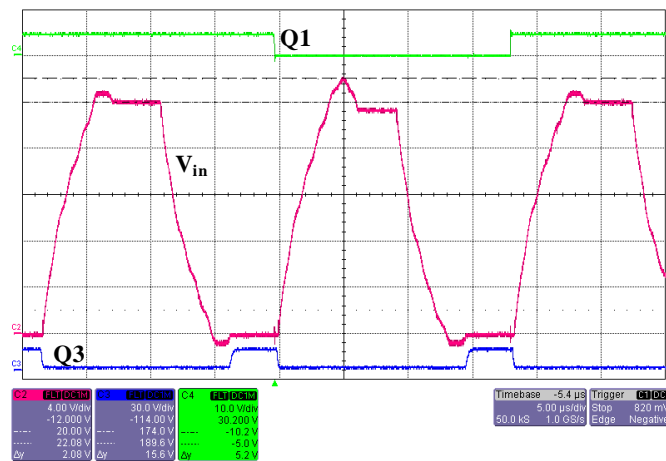

Figure 9: ZVS factor measurement of the prototype PT, with at capacitor ratio K_C of 2.16 (C_{d1} = 129nF). C3 and C4 shows gate signals, and C2 is the input voltage [4V/div].

Two sets of ZVS factor measurements have been collected through the experimental work. The approach in the experimental work has been to make a stepwise increment of the input capacitor C_{d1} and measure the drop in ZVS factor,

just as the parametric sweep performed in the simulations. The tests have been performed with two different half-bridge supply voltages, 10V and 20V, as the increase in voltage should reflect a decrees in efficiency. This is due to the nonlinear nature of the piezoelectric loss.

Figure 10 illustrates the test results and it can be observed that the measurements are not as linear as anticipated, but the test setup also involved a certain measurement inaccuracy. But just as expected the ZVS factor drops when employing a higher half-bridge supply voltage.
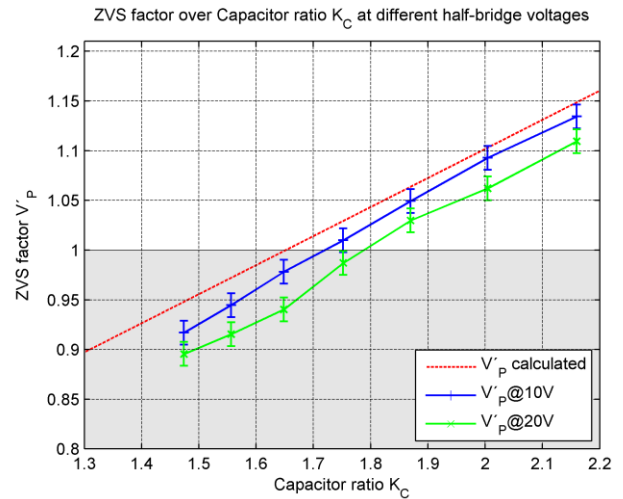

Figure 10: ZVS factor measurement of prototype PT in relation to the capacitor ratio K_C, compared with the ZVS factor equation.

5 Discussion

Comparing the predictions of the developed ZVS factor Equation (5) with the results extracted from the simulations, there is a very good correlation as illustrated in Table 3, where an accuracy below 1% is demonstrated. As for the results obtained through the experimental work Figure 10, it reveals that the ZVS factor is a bit more optimistic than the results. This is mainly due to the fact that the PT efficiency drops when the half-bridge voltage is increased. And as the lumped parameters of Table 4 are extracted from small-signal impedance measurements, the efficiency is also a measure of efficiency at small signals. The ZVS factor predictions of Figure 10 are based on this efficiency, so it is obvious that it will be a bit optimistic. Basically the efficiency used for the prediction should be modified as the working point changes to 10V and 20V. This is quite difficult though, because of the lack of a good and reliable efficiency measurement method. This is due to the high frequency AC load and standard power analysers are typically optimised for DC or low frequency 50/60Hz AC mains. Taking a closer look at Figure 10 it can be seen that the results are not as linear as expected, nor parallel to the predicted ZVS factor. However just looking at the result with a ZVS factor above 1, they are quite linear and parallel to the predicted ZVS factor. Some of the deviation could defiantly be due to measurement inaccuracy, as the measurements are extracted by hand, from oscilloscope plots as Figure 8 and Figure 9. Nonetheless the deviations could

also origin from elements in the circuit, which is not include in the idealised simulation, such as the highly nonlinearities of semiconductor parasitic capacitances. Although not taking the efficiency drop in to account, the developed ZVS factor manages to do a prediction within 3% of the 10V test results and within 6% of the 20V test results. As a final note it can be noted that a capacitor ration K_C of at least 1.55 is needed in order to achieve soft switching capability and a ZVS factor above 1.

6 Conclusion

Through a series of parametric sweep PSpice simulations an expression describing the maximal obtainable soft switching capability has been derived, also known as the ZVS factor. The expression is very simple and transparent, clearly stating the strong dependency of the input and output capacitor ratio, as well as the dependency of the efficiency. As a result the soft switching capability of a specific PT design can be evaluated easily and directly from the lumped parameter model. The ZVS factor forms a basic soft switching capability measuring tool, to assist through the development of ZVS optimised PT's. The developed ZVS factor has been evaluated up against the simulations as well as against a developed prototype DC/AC inductor-less half-bridge converter. It demonstrated below 1% accuracy compared to the simulations, validating its functionality. And a 3-6% accuracy compared to the prototype, bearing in mind that a too optimistic efficiency for calculating the ZVS factor were used.

Acknowledgements

References

[1] J. M. Alonso, C. Ordiz, M. A. D. Costa, J. Ribas, J. Cardesín, " High-Voltage Power Supply for Ozone Generation Based on Piezoelectric Transformer", *IEEE TRANSACTIONS ON INDUSTRY APPLICATIONS*, VOL. 45 NO. 4, 1513-1523 (2009)

[2] E. M. Baker,"Design of Radial Mode Piezoelectric Transformers for Lamp Ballast Applications", *PhD thesis*, Blacksburg Virginia (2002)

[3] S. Bronstein, S. Ben-Yaakov, "Design considerations for achieving zvs in a half bridge inverter that drives a piezoelectric transformer with no series inductor", *Power Electronics Specialists Conference, PESC 02*, vol. 2, pp. 585-590 (2002)

[4] W. R. Erikson, D. Maksimovié, [Fundamentals of Power Electronics], Springer Science+Business Media inc., (2001)

[5] E. L. Horsley, N. Nguyen-Quang, M.P. Foster, D. A. Stone, "Achieving ZVS in inductor-less half-bridge piezoelectric transformer based resonant converters", *PEDS*, 2009, 446-451

[6] E. L. Horsley, M. P. Foster, D. A. Stone, "State-of-the-art Piezoelectric Transformer Technology", *European Conference on Power Electronics and Applications*, 1-10 (2007)

[7] W. Huang, D. Chen, E. M. Baker, J. Zhou, H-I. Hsieh, F. C. Lee, "Design of a Power Piezoelectric Transformer for a PFC Electronic Ballast", *IEEE TRANSACTIONS ON INDUSTRIAL ELECTRONICS*, VOL. 54, NO. 6 (2007)

[8] C. Y. Lin, "Design and analysis of piezoelectric transformer converters," *PhD dissertation*, Blacksburg Virginia, (1997)

[9] F. L. CY. Lin, "Design of a piezoelectric transformer converter and its matching networks*", Power Electronics Specialists Conference*, PESC' 94 Record, (1994)

[10] R. L. Lin, "Piezoelectric Transformer Characterization and Application of Electronic Ballast", *PhD dissertation*, Blacksburg Virginia (2001)

[11] W. P. Mason, "Electromechanical Transducers and Wave Filters", D. Van Nostrand Co, (1942)

[12] K. S. Meyer, M. A. E. Andersen," Parameterized Analysis of Zero Voltage Switching in Resonant Converters for Optimal Electrode Layout of Piezoelectric Transformers*", PESC IEEE,* 978-1-4244-1668-4, 2543-2548 (2008)

[13] R. L. Lin, F. C. Lee, E. M. Baker, D. Y. Chen, "Inductor-less piezoelectric transformer electronic ballast for linear fluorescent lamp", *Applied Power Electronics Conference and Exposition*, vol.2, 664-669 (2001)

[14] M. S. Rødgaard, T. Andersen, K. S. Meyer, M. A. E. Andersen, "DESIGN OF INTERLEAVED MULTILAYER ROSEN TYPE PIEZOELECTRIC TRANSFORMER FOR HIGH VOLTAGE DC/DC APPLICATIONS", *Power Electronics, Machines and Drives Conference*, (2012)